Optimizing the paths for including the correction term to the hyperspherical hidden crossing method: Application to Ps formation in e^+-Li collisions

S. J. Ward,[1] J. Shertzer,[2] S. Yu. Ovchinnikov,[3] and J. H. Macek[3]
[1]*Department of Physics, University of North Texas, Denton, Texas 76203, USA*
[2]*Department of Physics, College of the Holy Cross, Worcester, Massachusetts 01610, USA*
[3]*Department of Physics and Astronomy, University of Tennessee, Knoxville, Tennessee 37996, USA and Oak Ridge National Laboratory, Oak Ridge, Tennessee 37831, USA*
(Received 31 August 2006; published 18 January 2007)

A correction term to the hyperspherical hidden crossing method (HHCM) was previously derived for large hyperradius R using the one-Sturmian theory. With the correction term, the HHCM potentials agree asymptotically with close-coupling channel potentials through order $1/R^2$. Here, we present an optimal pair of paths in the complex R plane for the inclusion of the correction term. With this new pair of paths, the correction term can be treated in a consistent way for the two levels associated with a transition. Using the new paths, we apply the HHCM with the correction term to calculate s-, p-, d-, and f-partial wave cross sections for Ps formation in e^+-Li collisions in the energy range 0–1.8 eV. The comparison of the total Ps formation cross section, with both an accurate hyperspherical close-coupling calculation and experimental measurements, shows that the HHCM with the correction term is a reliable method to describe collisions involving three charged particles. A systematic study of the Stückelberg phase with respect to orbital angular momentum and momentum of the incident positron provides interesting insights into the scattering process.

DOI: 10.1103/PhysRevA.75.012713 PACS number(s): 34.10.+x, 34.70.+e, 34.85.+x, 36.10.Dr

I. INTRODUCTION

The hyperspherical hidden crossing method (HHCM) was formulated to treat collisions involving three charged particles of arbitrary mass and charge [1]. Like the hyperspherical close-coupling (HSCC) method, the HHCM has the important feature that excitation and rearrangement channels can be treated on an equal footing. This is particularly advantageous for positron collisions, where Ps formation channels can be problematic. The HHCM can also provide valuable insight into scattering processes.

The HHCM has been applied to several collision systems [1–8]. It provided an interpretation of the minimum in the ionization cross section for electron impact of a $Z=1/4$ collinear model [2] and the minimum in the transition probability for the recombination of three identical bosons [3]. The HHCM cross sections for e^--H ionization [4] and electron excitation of hydrogen ($n=2$) [1] are accurate to about 10%. We previously applied the HHCM to compute partial wave Ps formation cross sections for both e^+-H collisions [5] and e^+-Li [6–8] collisions in the energy range where there are two open channels, elastic scattering and Ps formation. The HHCM provided an explanation for the extremely small s-wave Ps formation cross section for both collision systems.

The HHCM is not an exact method. A correction term to the HHCM potentials was derived for large hyperradius R [5] using the one-Sturmian theory [1]. With this correction term, the HHCM potentials agree asymptotically with the close-coupling potentials to order $1/R^2$ [9]. In a previous calculation, we included the correction term for e^+-Li collisions and computed partial wave Ps formation cross sections [6–8]. This calculation demonstrated the importance of the correction term; in general the Ps formation cross sections were reduced, bringing them into closer agreement with other calculations [10–14]. However, there were unphysical irregularities in the cross sections [6–8].

In this paper, we show how to include the correction term to the HHCM so that the resulting cross sections are free of these unphysical irregularities. For the case where there are two open channels, there are two paths in the complex R plane for a transition from one level i to the other level j. We choose an optimal pair of paths which has advantage that the correction term can be included in a consistent way for the two levels. We stress that the method for optimizing the paths for including the correction term is entirely general and applicable to any collision involving three charged particles. We refer to the calculations that include the correction term for the optimal pair of paths as HHCM$^{+\mathrm{cor}}$.

Using the correction term with the new paths, we recalculate the partial wave cross sections for Ps formation in e^+-Li collisions in the energy range where there are only two open channels (0–1.8 eV). We find that using the new paths not only leads to cross sections that are free of unphysical irregularities but also greatly improves the overall accuracy of the results. The HHCM$^{+\mathrm{cor}}$ total Ps formation cross section compares favorably with an accurate HSCC calculation [14] and with experimental measurements [15]. A systematic study of the Stückelberg phase with respect to orbital angular momentum and momentum of the incident positron provides interesting insights into the scattering process.

In Sec. II, we present the details of the implementation of the correction term and describe the optimal pair of paths. In Sec. III, we apply the HHCM$^{+\mathrm{cor}}$ to Ps formation in e^+-Li collisions; the results of the cross sections are presented in Sec. IV. In Sec. V, we discuss our findings concerning the Stückelberg phase for e^+-Li collisions and review other atomic processes where the Stückelberg phase is a multiple of π. We give the concluding remarks in Sec. VI. Atomic units are used throughout unless explicitly stated.

II. INCLUDING THE CORRECTION TERM TO THE HHCM

We briefly outline the HHCM in order to place in context the discussion on the choice of paths for including the correction term [5] that was derived from the one-Sturmian approximation [1].

The HHCM is formulated using the hyperspherical coordinates [1]. The hyperspherical coordinates for positron-atom collisions are the hyperradius $R=\sqrt{r_+^2+r_-^2}$ and the hyperangles $\alpha=\tan^{-1}\left(\frac{r_-}{r_+}\right)$ and $\theta=\cos^{-1}(\hat{\mathbf{r}}_+\cdot\hat{\mathbf{r}}_-)$, where $\mathbf{r}_+$ and $\mathbf{r}_-$ are the position vectors of e^+ and e^- with respect to the (infinitely heavy) nucleus, respectively [16]. The reduced wave function $\Psi(R,\Omega)$ is related to the Schrödinger wave function $\psi(R,\Omega)$ by $\Psi(R,\Omega)=R^{5/2}\sin\alpha\cos\alpha\psi(R,\Omega)$, where Ω represents the hyperangles α, θ, and the Euler angles ω_1, ω_2, and ω_3. The Schrödinger equation is expressed as

$$\left[-\frac{\partial^2}{\partial R^2}+\frac{\Lambda^2+2RC(\alpha,\theta)}{R^2}-2E\right]\Psi(R,\Omega)=0, \tag{1}$$

where $C(\alpha,\theta)$ is the reduced potential and E is the total energy of the three interacting particles. In this equation, the grand angular momentum operator Λ^2 is given by

$$\Lambda^2=-\frac{\partial^2}{\partial\alpha^2}+\frac{\mathbf{L}_+^2}{\cos^2\alpha}+\frac{\mathbf{L}_-^2}{\sin^2\alpha}-\frac{1}{4}. \tag{2}$$

The hyperspherical adiabatic basis function $\varphi_\mu(R;\Omega)$ are found by holding R fixed and solving

$$[\Lambda^2+2RC(\alpha,\theta)]\varphi_\mu(R;\Omega)=2\varepsilon_\mu(R)R^2\varphi_\mu(R;\Omega). \tag{3}$$

Using Demkov's construction [17], the adiabatic eigenfunctions $\varepsilon_\mu(R)$ are considered to be different branches of $\varepsilon(R)$, which is single valued function on a multisheeted Riemann surface. Two connecting sheets are joined at a branch point, and circling the branch point takes you from one sheet to the other.

The adiabatic function $\varphi_\mu(R;\Omega)$ is expanded into states of total angular momentum L [16]:

$$\varphi_\mu(R;\Omega)=\sum_{I=0}^{L}f_I(R;\alpha,\theta)\mathcal{D}^{(L)}_{|I|,M}(\omega_1,\omega_2,\omega_3). \tag{4}$$

The functions $f_I(R;\alpha,\theta)$ are solutions to the coupled partial differential equations,

$$\sum_{J=0}^{L}\mathcal{H}_{I,J}f_J(R;\alpha,\theta)=2R^2\varepsilon'_\mu(R)f_I(R;\alpha,\theta),\quad I=0,1,2\ldots.L, \tag{5}$$

where the operators $\mathcal{H}_{I,J}$ are given in Refs. [16,18]. The eigenvalues $\varepsilon'_\mu(R)$ are related to the adiabatic eigenvalues $\varepsilon_\mu(R)$ of Eq. (3) by

$$\varepsilon'_\mu(R)=\varepsilon_\mu(R)+\frac{1}{2}\left(\frac{1}{4R^2}\right). \tag{6}$$

The wave vector used in the HHCM is defined in terms of these eigenvalues

$$K_\mu^2(R)=2[E-\varepsilon'_\mu(R)]. \tag{7}$$

(The L superscript for the wave vector and eigenvalues has been suppressed for brevity.)

Within the framework of the HHCM formalism, we can extract information about a transition between levels i and j by summing Wentzel-Kramers-Brillouin (WKB)-like functions of the form $e^{i\int K(R)dR}$ over the paths that connect levels i and j at large R. For the energy range where there are only two open channels, there are two paths that lead to the transition from level i to level j. The two paths are as follows. On the first path, one comes in from infinity on the negative branch of $K_i(R)=\sqrt{2(E-\varepsilon'_i(R))}$ to a point on the real axis that is less than or equal to the classical turning R_i^t on level i. This ensures that one does not cross the branch cut of $K_i(R)$ which is chosen from R_i^t to infinity along the real axis. One then encircles clockwise the branch point R_b in the upper half plane that connects levels i and j. Finally, one goes out to infinity along the positive branch of $K_j=\sqrt{2(E-\varepsilon'_j(R))}$. For the second path, one comes in from infinity on the negative branch of $K_i(R)$, encircles clockwise the branch point R_b^* in the lower half plane, and continues to a point less than or equal to the classical turning point R_j^t of level j. One then goes back out to infinity on the positive branch of $K_j(R)$. A discussion of the complex conjugate pair of branch points R_b and R_b^* is given in Refs. [19,20]. The modulus square of the sum of $e^{i\int K(R)dR}$ over the two paths is

$$\left|e^{i\int_{\text{path 1}}K(R)dR}+e^{i\int_{\text{path 2}}K(R)dR}\right|^2=4P_{ij}^L\cos^2\Delta_{ij}^L \tag{8}$$

where Δ_{ij}^L is the Stückelberg phase

$$\Delta_{ij}^L=\mathrm{Re}\int_c K(R)dR \tag{9}$$

and P_{ij}^L is the one-way transition probability

$$P_{ij}^L=\exp\left(-2\mathrm{Im}\int_c K(R)dR\right). \tag{10}$$

The contour c in Eqs. (9) and (10) starts at R_i^t, goes clockwise around R_b and ends at R_j^t. We note that integrating $K(R)$ along any two paths with the properties of the pair of paths described above will reduce to this contour integral c, provided that no other branch point in the Riemann surface of $\varepsilon(R)$ is enclosed. (Ostrovsky [21] considered a similar contour in his calculation of the Stückelberg phase for $L=0$ $dt\mu$ rearrangement. He integrated along a closed contour that encircles both R_b and R_b^* and loops around the turning points of the initial and final sheets to obtain twice the Stückelberg phase.)

To obtain $|S_{ij}|^2$ a phase of $\frac{\pi}{2}$ is added to the Stückelberg phase in Eq. (8); this accounts for the change in sign of the adiabatic function $\varphi_\mu(R;\Omega)$ upon two turns around a branch point [1]. This results in

$$|S_{ij}^L|^2=4P_{ij}^L\sin^2\Delta_{ij}^L. \tag{11}$$

As is standard, to ensure unitary, Eq. (11) is multiplied by the factor $(1-P_{ij}^L)$,

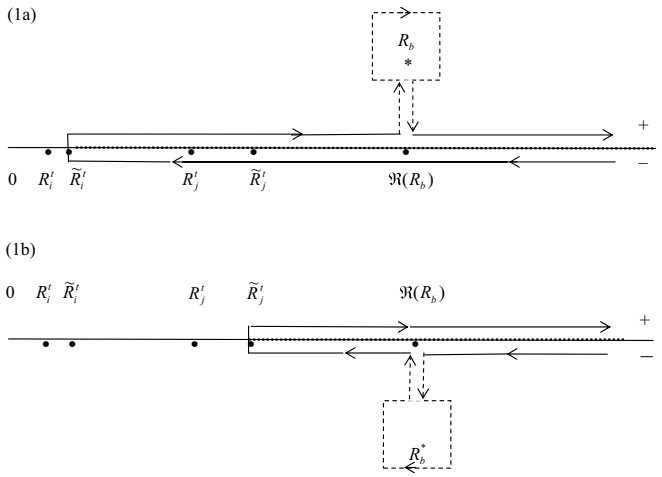

FIG. 1. Pair of paths that were used in the previous calculation of the HHCM with correction term. The dashed-line shows where $K(R)$ of Eq. (7) is used. The solid line shows where $\tilde{K}(R)$ of Eq. (15) is used. The horizontal dotted line shows the branch cut of the wave vector. The +/– sign denotes the positive/negative branch of the wave vector. The arrows indicates the direction that the contour is transversed. (a) Path around R_b. (b) Path around R_b^*.

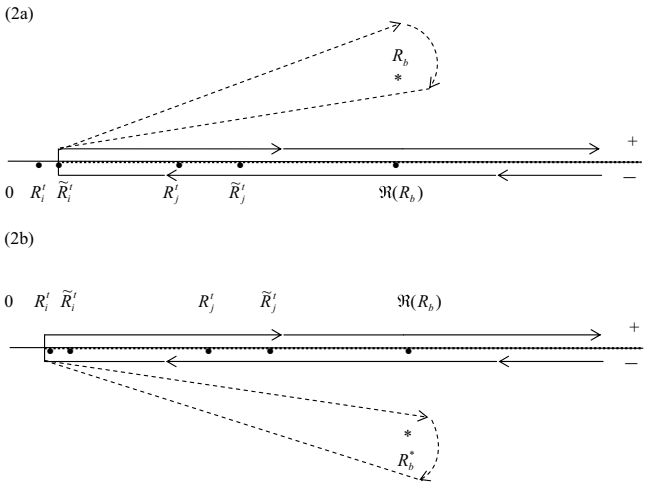

FIG. 2. Optimal pair of paths for the HHCM^{+cor} calculation. The dashed-line shows where $K(R)$ of Eq. (7) is used. The solid-line shows where $\tilde{K}(R)$ of Eq. (15) is used. The horizontal dotted line shows the branch cut of the wave vector. The +/– sign denotes the positive/negative branch of the wave vector. The arrows indicates the direction that the contour is transversed. (a) Path around R_b. (b) Path around R_b^*.

$$|\tilde{S}_{ij}^L|^2 = 4P_{ij}^L(1-P_{ij}^L)\sin^2\Delta_{ij}^L. \tag{12}$$

The justification for the factor $(1-P_{ij}^L)$ can be found in Refs. [20,22]. In terms of $|\tilde{S}_{ij}^L|^2$, the partial wave cross section for the transition between levels i and j (in units of πa_0^2) is given by

$$\sigma_{ij}^L = \frac{(2L+1)}{k_i^2}|\tilde{S}_{ij}^L|^2, \tag{13}$$

where k_i is the momentum of the particle coming in on level i.

Using the one-Sturmian theory [1], one can derive a correction term to the potential $\varepsilon'(R)$ when $\varepsilon'(R)$ is a slowly varying function of R, which is the case for large R [5]. The potential with the correction term,

$$\tilde{\varepsilon}'_\mu(R) = \varepsilon'_\mu(R) - \frac{1}{2}\left[\frac{1}{4R^2} + \left\langle \varphi_\mu \middle| \frac{\partial^2\varphi_\mu}{\partial R^2}\right\rangle\right]$$
$$= \varepsilon_\mu(R) - \frac{1}{2}\left\langle \varphi_\mu \middle| \frac{\partial^2\varphi_\mu}{\partial R^2}\right\rangle, \tag{14}$$

agrees asymptotically with the close-coupling channel potentials through terms of order $1/R^2$ [9]. It is important, therefore, to include the correction term for large real R. The wave vector $\tilde{K}_\mu^2(R)$ corresponding to the potential with the correction term is

$$\tilde{K}_\mu^2(R) = 2(E - \tilde{\varepsilon}'_\mu(R)). \tag{15}$$

The correction term diverges at the branch point. Therefore, we do not include the correction term off the real axis.

In our earlier calculations of Ps formation in e^+-Li collisions [6–8], we included the correction term along the real axis for the two paths shown in Figs. 1(a) and 1(b). The contour integral $\int_c K(R)dR$ in Eqs. (9) and (10) is replaced by the contour integral $\int_{\tilde{R}_i^t}^{\mathrm{Re}(R_b)} \tilde{K}_i(R)dR + \int_{c'} K(R)dR + \int_{\mathrm{Re}(R_b)}^{\tilde{R}_j^t} \tilde{K}_j(R)dR$, where c' is the contour loop that starts at $\mathrm{Re}(R_b)$, encircles clockwise R_b, and returns to $\mathrm{Re}(R_b)$. $\tilde{R}_i^t$ and $\tilde{R}_j^t$ are the classical turning points of the potentials $\tilde{\varepsilon}'_i(R)$ and $\tilde{\varepsilon}'_j(R)$, respectively. We found that including the correction term in general lowered the p-, d-, and f-wave HHCM cross sections for Ps formation in e^+-Li collisions, and brought them into closer agreement with the Kohn variational results [10–12]. The calculations, therefore, confirmed the importance of the correction term. However, for this choice of paths including the correction term along the real axis resulted in unphysical irregularities in some of the partial wave cross sections. These irregularities occured over the energy range where $R_j^t < \mathrm{Re}(R_b) < \tilde{R}_j^t$, where $\mathrm{Re}(R_b)$ is the point where one leaves the real axis to encircle the branch point. For this energy range, there is some inconsistency in the contour integral when one includes the correction term along the real axis.

In this paper, we show how to implement the correction term in a consistent way for both levels for the two paths; the cross sections do not have the unphysical irregularities present in the previous calculations. We include the correction term along the real axis for paths 1 and 2 which we show, respectively, in Figs. 2(a) and 2(b). For path 1, using the negative branch of $\tilde{K}_i(R)$, one integrates $\tilde{K}_i(R)$ from infinity to $\tilde{R}_i^t$, and then one integrates $K(R)$ along a contour that starts at $\tilde{R}_i^t$ goes clockwise around the branch point R_b and returns to $\tilde{R}_i^t$. Finally, using the positive branch of $\tilde{K}_j(R)$, one integrates $\tilde{K}_j(R)$ outwards to infinity. Path 2 is similar, except that one integrates along a loop that goes clockwise around

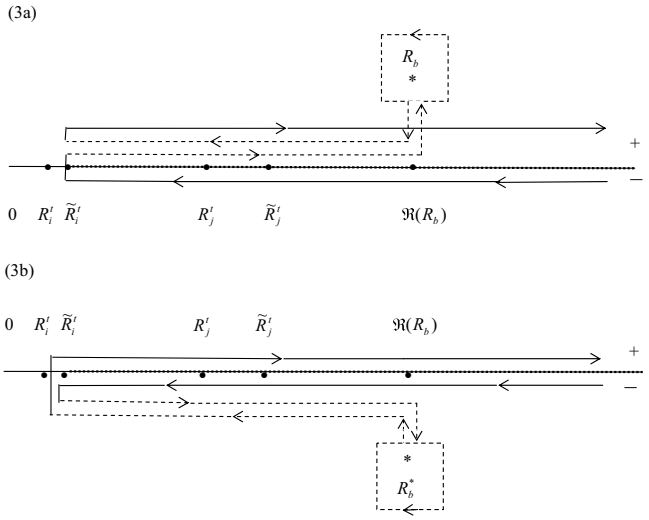

FIG. 3. Pair of paths equivalent to those shown in Fig. 2, deformed for purposes of the calculation. The dashed line shows where $K(R)$ of Eq. (7) is used. The solid-line shows where $\tilde{K}(R)$ of Eq. (15) is used. The horizontal dotted line shows the branch cut of the wave vector. The +/– sign denotes the positive/negative branch of the wave vector. The arrows indicates the direction that the contour is transversed. (a) Path around R_b. (b) Path around R_b^*.

R_b^*, rather than around R_b. For both paths, the point where one returns to the real axis after encircling the branch point, $\tilde{R}_i^t$, is always less than both R_j^t and $\tilde{R}_j^t$. Hence, the cross section will be free of the irregularities that appeared in the previous calculation.

For the practical calculation, we deform the contours of these two paths to ensure that only the branch point between levels i and j is included. We show the deformed paths in Figs. 3(a) and 3(b). For these paths, $|\tilde{S}_{ij}|^2$ for the transition between levels i and j is given by Eq. (12) where now the Stückelberg phase is given by

$$\Delta_{ij}^L = \mathrm{Re}\int_{\tilde{c}} K(R)dR \tag{16}$$

and the one-way transition probability by

$$P_{ij}^L = \exp\left(-2\mathrm{Im}\left(\int_{\tilde{c}} K(R)dR - \int_{\tilde{R}_i^t}^{R_j^t} K_j(R)dR + \int_{\tilde{R}_i^t}^{\tilde{R}_j^t} \tilde{K}_j(R)dR\right)\right). \tag{17}$$

The contour $\tilde{c}$ starts at $\tilde{R}_i^t$, encircles R_b, and ends at R_j^t. We refer in this paper to the calculation that uses $|\tilde{S}_{ij}|^2$ of Eq. (12) with the Stückelberg phase of Eq. (16) and the one-way transition probability of Eq. (17) as the HHCM with correction term (HHCM$^{+\mathrm{cor}}$). Clearly, without the correction term, Eqs. (16) and (17) reduce, respectively, to Eqs. (9) and (10) of the HHCM calculation. Since $\tilde{R}_i^t$ is close to R_i^t, the Stückelberg phase given by Eq. (16) is almost identical to the Stückelberg phase given by Eq. (9). It is interesting that, unlike the earlier calculations with the correction term using the old paths, the integral for the Stückelberg phase involves only $K(R)$. The probability, on the other hand, involves both $K(R)$ and $\tilde{K}(R)$.

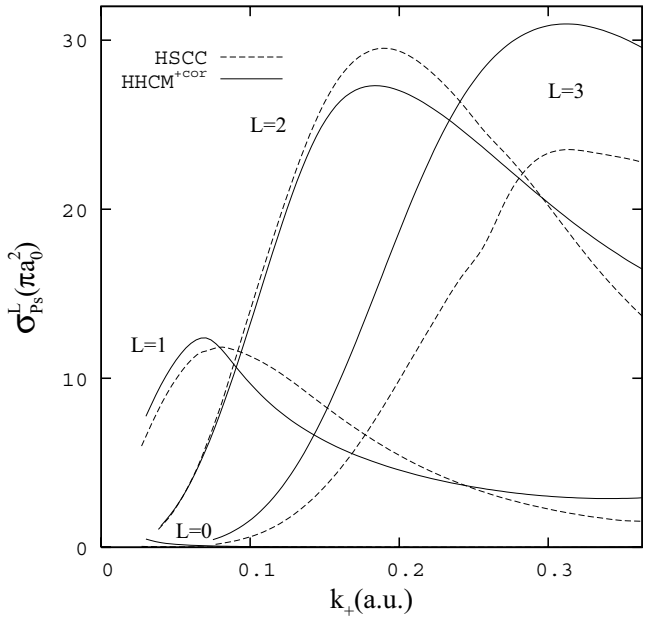

FIG. 4. The HHCM$^{+\mathrm{cor}}$ partial wave cross sections for Ps formation in e^+-Li collisions are compared with HSCC results. In both cases, the $L=0$ cross section is very small.

III. APPLICATION TO e^+-Li COLLISIONS

The HHCM (with correction term) can be applied to positron–alkali-metal-atom collisions by treating the alkali atom as an effective one-electron atom. For the alkali-metal atoms, the interaction of the valence electron with the core is well represented by a model potential.

In this paper, we apply the HHCM$^{+\mathrm{cor}}$ to Ps formation in e^+-Li collisions. We compute the s-, p-, d-, and f-wave cross sections for Ps formation in the energy range 0–1.8 eV. In this energy range there are only two open channels, elastic scattering and Ps formation. We use the parametric model potential developed by Peach [23] where the effective e^-Li$^+$ interaction is

$$V_{e^-\mathrm{Li}^+}(\mathbf{r}_-) = -\frac{1}{r_-} - \frac{2e^{-\gamma r_-}}{r_-}(1+\delta r_- + \delta' r_-^2) - \frac{\alpha_d}{2r_-^4} w_2(\beta r_-). \tag{18}$$

The first two terms in this equation represent the static interaction and the third represents the core polarization. The value of the static dipole polarizability of the core α_d is 0.192 456 [24]. The cut-off function $w_2(x)$ is given by

$$w_2(x) = \left[1 - e^{-x}\left(1 + x + \tfrac{1}{2}x^2\right)\right]^2. \tag{19}$$

The empirical parameters γ, δ, δ', and β were optimized to reproduce the spectroscopic energy levels and to ensure that Li($2s$) had the correct nodal structure [23]. The fit to the

spectroscopic energy levels is excellent. The model potential does give rise to a spurious Li($1s$) state. However, because this state is so tightly bound ($E=-1.892\,766$) and far below the energy of the physical Li($2s$) state ($E_{\mathrm{Li}}=-0.197\,952$), it causes no practical problems in scattering or bound state calculations.

For the $e^+\mathrm{Li}^+$ interaction, we use

$$V_{e^+\mathrm{Li}^+}(\mathbf{r}_+)=\frac{1}{r_+}+\frac{2e^{-\gamma r_+}}{r_+}(1+\delta r_+ +\delta' r_+^2)-\frac{\alpha_d}{2r_+^4}w_2(\beta r_+). \tag{20}$$

The e^+e^- interaction is given by

$$V_{e^+e^-}(\mathbf{r}_+,\mathbf{r}_-)=-\frac{1}{|\mathbf{r}_+-\mathbf{r}_-|}+\frac{\alpha_d}{r_-^2 r_+^2}\cos\theta\sqrt{w_2(\beta r_+)w_2(\beta r_-)}. \tag{21}$$

The second term in Eq. (21) is analogous to the dielectronic correction. It ensures that there is no core polarization when the electron and positron coalesce. The Peach model potential implicitly includes exchange effects that are not present for the $e^+\mathrm{Li}^+$ interaction. In order to test the validity of using this model potential for the e^+Li system, we calculated the binding energy of the weakly bound-state of e^+Li [25] using Eqs. (18), (20), and (21). The binding energy is in excellent agreement with calculations using the exact five-body Hamiltonian [26,27].

As a result of using a model potential to describe the Li^+ core, the reduced potential of Eq. (3) now depends explicitly on the hyperradius R in addition to the variables α and θ,

$$\begin{aligned}C(R;\alpha,\theta)=&\frac{1}{\cos\alpha}[1+2e^{-\gamma R\cos\alpha}(1+\delta R\cos\alpha+\delta' R^2\cos^2\alpha)]-\frac{\alpha_d}{2R^3\cos^4\alpha}w_2(\beta R\cos\alpha)\\&-\frac{1}{\sin\alpha}[1+2e^{-\gamma R\sin\alpha}(1+\delta R\sin\alpha+\delta' R^2\sin^2\alpha)]-\frac{\alpha_d}{2R^3\sin^4\alpha}w_2(\beta R\sin\alpha)\\&-\frac{1}{[1-\sin 2\alpha\cos\theta]^{1/2}}+\frac{\alpha_d}{R^3\sin^2\alpha\cos^2\alpha}\cos\theta\sqrt{w_2(\beta R\sin\alpha)w_2(\beta R\cos\alpha)}.\end{aligned} \tag{22}$$

The total energy of the e^+-Li system is $E=\frac{1}{2}k_+^2+E_{\mathrm{Li}}$, where k_+ is the momentum of the incoming positron and E_{Li} is the ground-state energy of the Li atom. The first three hyperspherical levels asymptotically correspond to e^+-Li($1s$), Ps($1s$)-Li^+, and e^+-Li($2s$), respectively.

IV. RESULTS: Ps FORMATION CROSS SECTION IN e^+-Li COLLISIONS

In Fig. 4 we compare the HHCM$^{+\mathrm{cor}}$ s-, p-, d-, and f-wave partial wave cross sections for Ps formation in e^+-Li collisions with HSCC results [14]. The HSCC calculation also includes the core polarization. In both calculations, the s-wave Ps formation cross section is very small. The HHCM$^{+\mathrm{cor}}$ p- and d-wave cross sections for Ps formation are in good agreement with the HSCC results. The HHCM$^{+\mathrm{cor}}$ f-wave cross section is larger than the HSCC result because $\tilde{R}_i^t$ is larger than is it for the lower partial waves and therefore the integration range for the integral of $\tilde{K}_j(R)$ is smaller. Consequently, the correction term will have a less of an effect in reducing the probability and the cross section. The HHCM$^{+\mathrm{cor}}$ cross sections do not have the unphysical irregularities that were present in the previous calculations with the correction term [6–8]. Furthermore, using the optimal paths to include the correction term has greatly improved the accuracy of the partial wave cross sections.

In Fig. 5, we compare the HHCM$^{+\mathrm{cor}}$ and HHCM total cross sections for Ps formation (summed over the four lowest partial waves) with HSCC [14] and experimental measurements [15]. For the HSCC, we show the total cross section for Ps formation where the sum is over the four lowest partial waves and also the cross section where the partial wave sum is up to $L=30$ [14]. The measurements are the lower limit to the Ps formation cross section [15]. The comparison of the HHCM$^{+\mathrm{cor}}$ and HHCM cross sections with HSCC ($0\leqslant L\leqslant 3$) shows that including the correction term in the calculation greatly improves the accuracy of the cross section, bringing it into reasonably good agreement with the corresponding HSCC result over the entire energy range. The agreement between the HHCM$^{+\mathrm{cor}}$ and HSCC ($0\leqslant L\leqslant 3$) cross sections is excellent up to about 0.5 eV ($k_+\approx 0.19$). It is evident from the HSCC calculation that the four lowest partial waves give the major contribution to the Ps formation cross section for most of the energy range, up to $E\approx 1.2$ eV. The agreement of the HHCM$^{+\mathrm{cor}}$ with experiment is reasonable, especially at lower energies.

V. COMMENTS ON THE STÜCKELBERG PHASE

The interpretation of the very small s-wave cross section for e^+-Li collisions is provided by the HHCM [6–8] and HHCM$^{+\mathrm{cor}}$ calculations. Figure 6 shows the Stückelberg

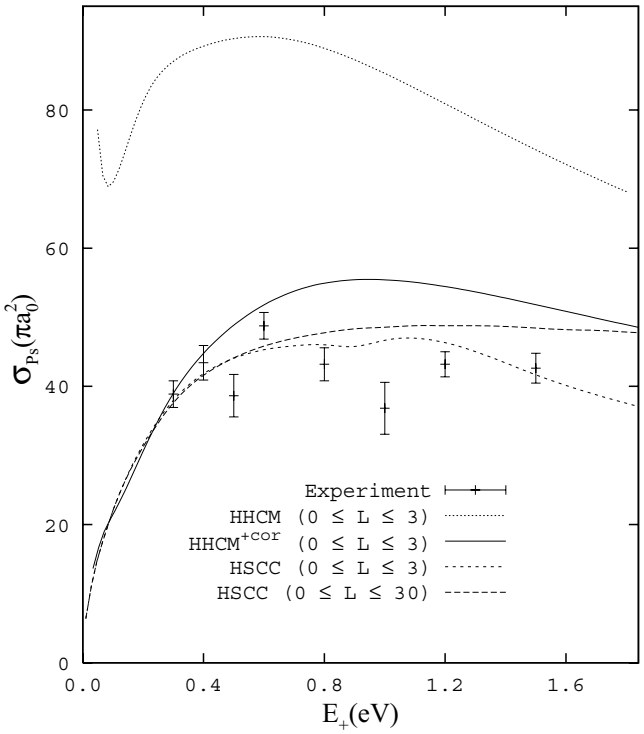

FIG. 5. A comparison of the HHCM^{+cor} ($0 \leqslant L \leqslant 3$) and the HHCM ($0 \leqslant L \leqslant 3$) total cross sections for Ps formation in e^+-Li collisions with HSCC ($0 \leqslant L \leqslant 3$ and $0 \leqslant L \leqslant 30$) and experimental measurements.

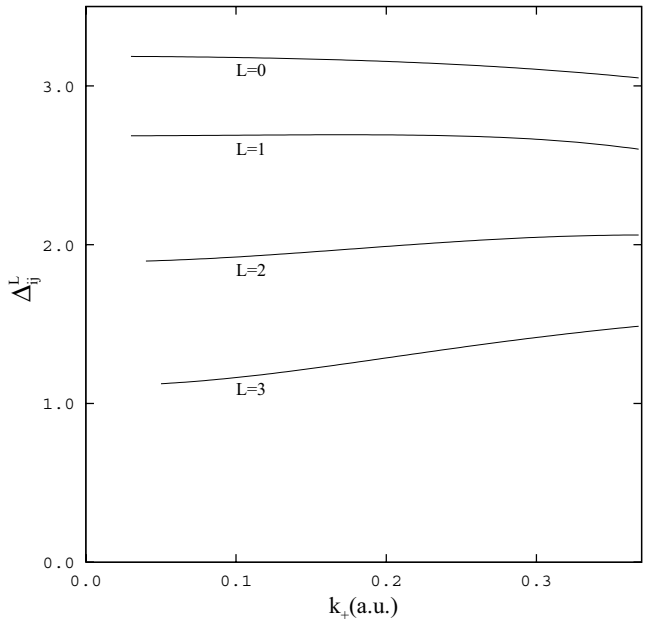

FIG. 6. The Stückelberg phase Δ_{ij}^L for partial waves $L=0$, 1, 2, and 3 vs the momentum of the incident positron.

phase for different L; the s-wave Stückelberg phase is close to π over the entire energy range, and passes through π at $k_+ \approx 0.23$. This means that the amplitudes corresponding to two different paths leading to Ps formation destructively interfere. At $k_+ \approx 0.23$, where the Stückelberg phase is exactly π, there is a minimum in the cross section. The f-wave Stückelberg phase is close to $\frac{\pi}{2}$ near the Ps($n=2$) threshold ($k_+ \approx 0.368$) which means that there is almost complete constructive interference between the amplitudes corresponding to two different paths leading to Ps formation. Near $k_+ \approx 0.24$, the f-wave becomes the dominant contribution to the total Ps formation cross section.

The Stückelberg phase varies in a systematic way with increasing L. For a given L, the Stückelberg phase varies fairly slowly with energy. The s- and p-wave Stückelberg phases decrease with k_+, but the d- and f-wave phases increase. From the systematic trend of the Stückelberg phase with L, one can predict that the g- and h-wave Stückelberg phases will be small and, consequently, their contributions to the Ps formation cross section will be less than the contributions from the d- and f-waves. This finding is consistent with the HSCC calculation which showed that the four lowest partial waves account for most of the contribution to the total Ps formation cross section.

It is interesting that the s-wave Stückelberg phase is close to π for Ps formation in e^+-Li collisions since this phase is also close to π for Ps formation in e^+-H collisions [5]. In both collision systems, the s-wave Ps formation cross section is very small due to destructive interference. Using the Kohn variational method, Van Reeth and Humberston [28] found that the s-wave cross section for Ps formation in e^+-He collisions in the Ore gap is very small. This suggests that the s-wave Stückelberg phase is a multiple of π for this collision system as well.

There are other $L=0$ collision systems in which the Stückelberg phase is a multiple of π. Ostrovsky [21] found that for $d\mu(1s)+t \rightarrow d+t\mu(1s)$ rearrangement process the Stückelberg phase is approximately 2π. Miyashita *et al.* [2] applied the HHCM to compute the transition probability for electron excitation ($n=1 \rightarrow 2$) of a collinear $Z=1/4$ model atom. A Stückelberg phase of π was obtained at a particular energy which gave a minimum in the transition probability. They used this result to interpret the minimum in *ab initio* calculations of electron-impact ionization of the model atom. Nielsen and Macek [3] showed that the minimum in the transition probability for the recombination of three identical bosons corresponds to where the Stückelberg phase is 3π.

VI. CONCLUSIONS

The correction term to the HHCM derived from the one-Sturmian theory is needed to ensure that the potentials used in the calculations agree asymptotically with the close-coupling channel potentials to order $1/R^2$. The optimal pair of paths enable the correction term to be included in a consistent way for the two levels associated with a transition. This means that the cross sections calculated with these paths are free of unphysical irregularities. Using the optimal pair of paths, we applied the HHCM with correction term to Ps formation in e^+-Li collisions. We found that the total cross section for Ps formation is in reasonable agreement with both HSCC and experimental measurements. The calculation suggests that the HHCM^{+cor} is a viable method to describe collisions involving three charged particles.

ACKNOWLEDGMENTS

We are grateful to Dr. Anh Thu Le for discussions and for providing us with tables of the HSCC cross sections. S.J.W. and J.S. acknowledge support from the National Science Foundation, under a collaborative grant (PHYS-0440714, PHYS-0440565). J.H.M. and S.Y.O. acknowledge support by the Chemical Science, Geosciences and Biosciences Division, Office of Basic Energy Sciences, Office of Science, U.S. Department of Energy under Grant No. DE-FG02-02ER15283. Oak Ridge National Laboratory is managed by UT Battle LCC under contract number DE-AC05-00OR22725. S.J.W. acknowledges the use of the UNT academic computing facilities. J.S. appreciates the hospitality at the Institute for Theoretical Atomic and Molecular Physics at the Harvard University and Smithsonian Astrophysical Observatory.

[1] J. H. Macek and S. Yu. Ovchinnikov, Phys. Rev. A **54**, 544 (1996).
[2] Naoyuki Miyashita, Shinichi Watanabe, Michio Matsuzawa, and Joseph H. Macek, Phys. Rev. A **61**, 014901 (1999).
[3] Esben Nielsen and J. H. Macek, Phys. Rev. Lett. **83**, 1566 (1999).
[4] J. H. Macek, S. Yu. Ovchinnikov, and S. V. Pasovets, Phys. Rev. Lett. **74**, 4631 (1995).
[5] S. J. Ward, J. H. Macek, and S. Yu. Ovchinnikov, Phys. Rev. A **59**, 4418 (1999).
[6] S. J. Ward and J. Shertzer, Phys. Rev. A **68**, 032720 (2003).
[7] S. J. Ward and J. Shertzer, Nucl. Instrum. Methods Phys. Res. A **221**, 206 (2004).
[8] S. J. Ward and J. Shertzer, Nucl. Instrum. Methods Phys. Res. A **241**, 257 (2005).
[9] M. Cavagnero, Z. Zhen, and J. Macek, Phys. Rev. A **41**, 1225 (1990).
[10] M. S. T. Watts and J. W. Humberston, J. Phys. B **25**, L491 (1992).
[11] J. W. Humberston and M. S. T. Watts, Hyperfine Interact. **89**, 48 (1994).
[12] M. S. T. Watts, Ph.D. thesis, University of London, 1994.
[13] A. A. Kernoghan, M. T. McAlinden, and H. R. J. Walters, J. Phys. B **27**, L625 (1994).
[14] Anh-Thu Le, M. W. J. Bromley, and C. D. Lin, Phys. Rev. A **71**, 032713 (2005); and Anh-Thu Le, private communication.
[15] E. Surdutovich, J. M. Johnson, W. E. Kauppila, C. K. Kwan, and T. S. Stein, Phys. Rev. A **65**, 032713 (2002).
[16] Yan Zhou and C. D. Lin, J. Phys. B **27**, 5065 (1994).
[17] Yu. N. Demkov, in *Proceedings of Invited Talks of the Fifth International Conference on the Physics of Electronic and Atomic Collisions, Leningrad, 1967*, edited by Lewis M. Branscomb, (Joint Institute for Laboratory Astrophysics, University of Colorado, Boulder, Colorado, 1968), p. 186.
[18] S. V. Passovets, J. H. Macek, and S. Yu. Ovchinnikov, in *The Physics of Electronic and Atomic Collisions*, edited by Louis. J. Dubé, J. Brian A. Mitchell, J. William McKonkey, and Chris E. Brion, AIP Conf. Proc. 360, (AIP, Woodbury, NY, 1995), p. 347.
[19] E. A. Solov'ev, Usp. Fiz. Nauk **157**, 437 (1989) [Sov. Phys. Usp. **32**, 228 (1989)].
[20] E. E. Nikitin and S. Ya. Umanskii, in *Theory of Slow Collisions* (Springer-Verlag, Berlin, 1984).
[21] V. N. Ostrovsky, Phys. Rev. A **61**, 032505 (2000).
[22] J. H. Macek and X. Y. Dong, Nucl. Instrum. Methods Phys. Res. B **42**, 475 (1989).
[23] G. Peach, H. E. Saraph, and M. J. Seaton, J. Phys. B **21**, 3669 (1988).
[24] R. M. Glover and F. Weinhold, J. Chem. Phys. **66**, 191 (1977).
[25] J. Shertzer and S. J. Ward, Phys. Rev. A **73**, 022504 (2006).
[26] Massimo Mella, Gabriele Morosi, and Darlo Bressanini, J. Chem. Phys. **111**, 108 (1999).
[27] J. Mitroy, Phys. Rev. A **70**, 024502 (2004).
[28] P. Van Reeth and J. W. Humberston, J. Phys. B **28**, L23 (1995).